IEEE Journal of Translational Engineering in Health and Medicine

Received 24 April 2017; revised 17 July 2017 and 7 August 2017; accepted 12 August 2017. Date of publication 4 September 2017; date of current version 21 September 2017.

*Digital Object Identifier 10.1109/JTEHM.2017.2740920*

# Managing Heart Failure at Home With Point-of-Care Diagnostics

**PAUL R. DEGREGORY[1], JANSEN TAPIA[1], TAMMY WONG[1], JO VILLA[1], IAN RICHARDS[2], AND RICHARD M. CROOKS[1]**

[1]Department of Chemistry, The University of Texas at Austin, Austin, TX 78712 USA
[2]Interactives Executive Excellence LLC, Austin, TX 78733 USA

CORRESPONDING AUTHOR: R. M. CROOKS (crooks@cm.utexas.edu)

This work was supported in part by the National Institutes of Health, National Heart, Lung, and Blood Institute under Grant R21HL128199, in part by the National Science Foundation I-Corps Program under Grant 1652746, and in part by the Robert A. Welch Foundation under Grant F-0032.

**ABSTRACT** The objective of this paper is development of an inexpensive point-of-care sensor for detecting the primary heart failure marker peptide, NT-proBNP. The device technology is based on an antibody sandwich assay, but with three innovative aspects. First, chemical amplification is carried out via oxidation of silver nanoparticles (NPs) attached to signaling antibodies rather than by enzymatic amplification. The electrochemical method is faster and eliminates the need for long-term storage of enzymes. Second, the antibody sandwich is formed on mobile magnetic beads. This enhances the rate of mass transfer of the biomarker and the signaling antibody to the primary detection antibody, which is immobilized on the magnetic beads. Third, the sensor itself is fabricated on a paper platform with screen-printed electrodes. This coupled with assembly by simple paper folding, keeps the cost of the sensor low. Here, we report on two separate assays. The first is based on a simple biotin-streptavidin conjugate, which is a preliminary model for the antibody assay. The results indicate a detection limit of 2.1 pM of silver NPs and an assay time of 7 min. The actual NT-proBNP antibody assay takes somewhat longer, and the dynamic detection range is higher: 2.9–582 nM. On the basis of the results presented in this paper, we conclude that this inexpensive paper-based sensor represents a viable technology for point-of-care testing of NT-proBNP, but nevertheless several challenges remain prior to clinical implementation. These include attaining a lower detection limit and better reproducibility, and optimizing the device for human blood.

**INDEX TERMS** Diagnostic device, heart failure, paper sensor, point of care technology.

## I. INTRODUCTION

### A. DEFINITION AND CHARACTERISTICS OF HF

This article focuses on the healthcare ecosystem surrounding heart failure (HF), and how a home-use, diagnostic tool for a HF biomarker that is being developed in our lab might fit into it. Testing for the biomarker, NT-proBNP, is already commonplace in centralized laboratories, and it is used, along with other tests, to rule in or rule out a diagnosis of HF. We believe that home testing of NT-proBNP, which can be viewed in some ways as analogous to diabetic blood glucose monitoring, could improve medical outcomes and reduce the cost of treating HF. This hypothesis is discussed within the broader context of home healthcare, the HF ecosystem, and finally the specific tool we are developing.

HF is a chronic disease comprising several complicating symptoms that conspire to reduce blood flow and hence provide insufficient oxygen to the body [1]. HF is subdivided into two general categories [2]. Diastolic HF is defined as the condition in which the left ventricle loses its ability to relax normally (because the muscle has become stiff), and therefore the heart can't properly fill with blood during the resting period between each beat. Systolic HF occurs when the left ventricle loses its ability to contract normally, so that the heart can't pump with enough force to push sufficient blood into circulation.

HF affects >5.8 million people in the U.S. and results in ∼1 million hospitalizations per year [1]. Although the underlying causes of the disease are not clear, several risk factors are associated with HF [3]. These include coronary artery disease, hypertension, and diabetes. Other risk factors include congenital heart defects, arrhythmias, myocarditis, cardiomyopathy, a previous heart attack, tobacco and alcohol use, and obesity. Extreme fatigue, shortness of breath (dyspnea), pulmonary edema, and fluid buildup in the lower extremities

(peripheral edema), resulting in weight gain, are some of the main symptoms of HF [4]. Typically, the condition is found in people over 65 years old, but it can affect people of any age [5]. It is more common in African Americans than in other racial groups [6]. HF can result in complicating conditions, such as kidney damage or failure, heart valve or rhythm problems, and depression [4].

Typically, dyspnea, and pulmonary and peripheral edema cause concern for patients and bring them into their doctor's office [7]. Diagnosis typically begins with a discussion of the patient's symptoms, a physical examination, and a review of the patient's medical history [4]. Physicians also usually check for the presence of risk factors, such as hypertension, coronary artery disease, and diabetes. Next, physicians may order blood tests, chest X-rays, electrocardiograms (ECGs), echocardiograms, stress tests, cardiac computerized tomography (CT) scans, or MRIs. The results of these tests not only help physicians diagnose HF, but they provide guidance for treatment. In acute exacerbations of HF, a patient's dyspnea may become so severe that the patient is compelled to visit the emergency room (ER) of a hospital [7]. Individuals with HF may also experience a condition known as paroxysmal nocturnal dyspnea (PND) [8]. PND causes patients wake in the night, due to their inability to breathe properly, and is said to be extremely frightening. In cases where a patient visits the ER with dyspnea, its cause may be unknown and an admitting physician may suspect either chronic obstructive pulmonary disease (COPD) or HF [9]. Clinical observation combined with diagnostic tests for specific biomarkers can help rule out HF.

The New York Heart Association (NYHA) has a symptom-based scale that classifies HF into four categories [10]. For Class I, there are no outward symptoms and no limitations on physical activity. In Class II HF, there are slight limitations on physical activity, and ordinary activities may result in fatigue or shortness in breath. Class III is more serious, and there are significant limitations on physical activity, and even minimal tasks will result in exhaustion and shortness of breath. Class IV is the most serious, and even at-rest patients suffer symptoms of HF.

The American College of Cardiology (ACC) and the American Heart Association (AHA) have developed a parallel classification system for HF [10]. In this formalism, stages A and B represent people who have not yet developed HF but are at high risk to do so because of coronary artery disease, high blood pressure, diabetes, or other predisposing conditions. Stage C includes individuals with past or current symptoms of HF who have a condition called structural heart disease. Stage D patients have advanced HF that is difficult to manage with standard treatment. Often, the NYHA and the ACC/AHA classification systems are used in tandem to guide therapy.

### B. BRAIN NATURIETIC PEPTIDE (BNP) AND NT-proBNP

BNP and NT-proBNP are two of several cardiovascular biomarkers in common use [11]. BNP is a hormone that acts as a diuretic and vasodilator, while the physiological significance of NT-proBNP is unknown. BNP and NT-proBNP are stored in cardiomyocytes as pre-ProBNP. During exacerbations of HF, blood volume overload in the heart chambers results in stretching of these cardiomyocytes. This stress triggers cleavage of pre-ProBNP to Pro-BNP inside the cardiomyocytes, and then Pro-BNP is enzymatically cleaved into BNP and NT-proBNP on its way through the cell membrane and into the bloodstream (Figure 1). Because BNP and NT-proBNP both originate from proBNP, they are present in a 1:1 ratio in blood and either peptide can be used to monitor HF. Compared to BNP, however, NT-proBNP has a longer circulation half-life [11] and higher stability [12] in samples collected from patients. NT-proBNP also has higher rule-in and rule-out cutoffs for HF [11]. For these reasons, we've opted to use NT-proBNP for HF monitoring.

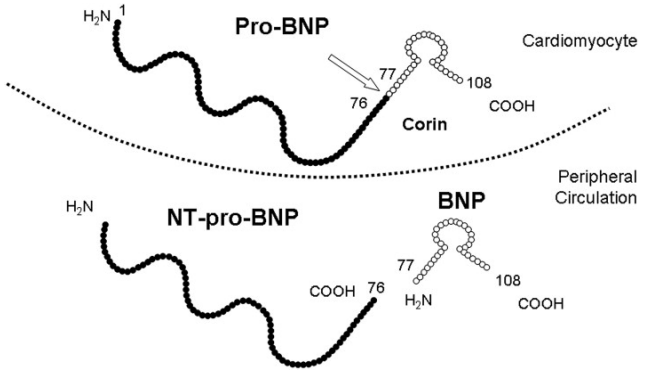


**FIGURE 1. NT-proBNP and BNP are produced in a 1:1 ratio after cleavage of Pro-BNP. Reprinted with permission from *J. Am. Coll. Cardiol: Cardiovascular Imaging* 2009, 2, 216-225. Copyright 2009 Elsevier.**

The NT-proBNP range to exclude HF is $<300$ pg/mL (35 pM), which has a negative predictive value of 99% [13], while levels $>900$ pg/mL (105 pM) are highly suggestive of HF. It is important to note that the NT-proBNP cutoff for diagnosing HF depends on age [14] and special situations, including patients' co-morbidity with renal failure [15] or obesity [16]. Our goal is to design an assay to identify NT-proBNP values at the inclusion, and optimally, exclusion, cutoff levels. Finally, NT-proBNP measurements resulting in a 25% or greater change from serial baseline readings are indicative of a worsening prognosis [17]. Therefore, regular home monitoring of NT-proBNP trends, independent of absolute levels, may prove useful.

## II. PROCEDURES AND RESULTS

### A. METHODS[1]

From the user perspective, the *No*Slip technology being developed in our lab is something like a home blood glucose sensor of the type used by diabetics. There are, however, two major differences. First, the *No*Slip detects NT-proBNP at low nanomolar levels compared to the low millimolar levels of glucose sensed by glucometers. Second, the much lower

[1]Part of the text in this section has been adapted with permission from ACS Sensors 2016, 1, 40-47, DOI: 10.1021/acssensors.5b00051. Copyright 2016 the American Chemical Society.

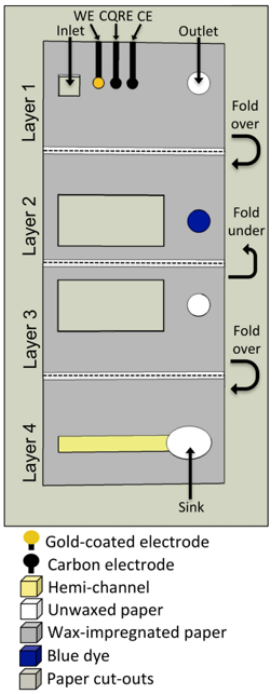


**FIGURE 2. A two-dimensional projection of the *No*Slip. See text for details. Reprinted with permission from *ACS Sensors* 2016, *1*, 40-47. (DOI: 10.1021/acssensors.5b00051). Copyright 2016 American Chemical Society.**

detection levels required for NT-proBNP require a different type of sensing mechanism.

The *No*Slip technology is a paper-based [18] electrochemical detection platform that provides a quantitative readout. The *No*Slip platform comprises four wax-printed paper layers, fabricated on a single piece of paper, that are subsequently folded to form the device [19]. As shown in Figure 2, Layer 1 contains two reservoirs, the inlet and the outlet. The inlet has its cellulose content removed while the outlet retains the unwaxed cellulose paper. In addition, three stencil-printed carbon electrodes are fabricated on the lower face of this layer (face in contact with Layer 2): the working electrode (WE), the carbon quasi-reference electrode (CQRE), and the counter electrode (CE).

A very thin layer of Au is deposited onto the surface of the carbon WE. During device operation, this Au will be oxidized to initiate galvanic exchange with silver nanoparticle (AgNP) labels (discussed next). Layers 2 and 3 contain hollow channels (i.e., the paper is cut out of this region) [20], and Layer 2 also has a paper reservoir loaded with a blue dye. This dye is used to signal cessation of flow through the hollow channels. Finally, Layer 4 consists of a hydrophilic layer (which we call a hemi-channel [21], yellow color) and a sink that drives a continuous flow of fluid through the device by capillary action. The *No*Slip is assembled by folding the paper as shown in Figures 2 and 3a to create a three-dimensional origami paper sensor.

As mentioned earlier, detection in the *No*Slip is carried out by a process called galvanic exchange. In galvanic exchange reactions, a zerovalent first metal reacts with the ions of a

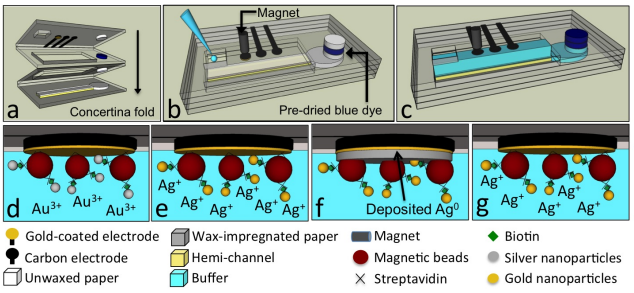


**FIGURE 3. Illustration of the operation of the *No*Slip. See text for details. Reprinted with permission from *ACS Sensors* 2016, *1*, 40-47. (DOI: 10.1021/acssensors.5b00051). Copyright 2016 American Chemical Society.**

second, more noble metal. If the redox potentials of the metals are sufficiently different, this results in oxidation of the first metal and reduction of the second. For *No*Slip detection, the first metal is the AgNP labels and the second metal ions are $Au^{3+}$. The relevant redox reaction is given by eq. 1.

$$3Ag_{(s)} + Au^{3+}_{(aq)} \rightarrow 3Ag^{+}_{(aq)} + Au_{(s)} \quad (1)$$

The approximate driving force for eq. 1 is the difference in the standard potentials of the individual half reactions: $\Delta E = 0.70$ V [22]. This is more than sufficient overpotential to drive eq. 1 to completion.

### *B. RESULTS*[2]

Preliminary tests of the *No*Slip were carried out using a model analyte consisting of 20 nm AgNP labels linked to ~2 $\mu$m magnetic microbeads (M$\mu$Bs) via biotin-streptavidin conjugation. We call this the M$\mu$B-AgNP composite. The general operation of the *No*Slip is illustrated in Figure 3. Once the device is assembled (Figure 3a), the sample (contained in chloride-containing buffer and having a volume of ~50 $\mu$L) is loaded at the inlet (Figure 3b). Capillary flow, driven by the hydrophilic floor of the channel (the hemi-channel) commences immediately, moving the sample down the open channel toward the sink (Figure 3c). The M$\mu$B-AgNP composite is localized under the working electrode (WE) by the magnet as the sample moves down the channel. As the sink fills with liquid, upward flow is initiated through the paper reservoir at the end of Layer 3 and toward the outlet. This rehydrates the dye on Layer 2 and a blue color appears at the outlet indicating that flow has stopped (Figure 3c) and that galvanic exchange detection can be initiated.

Figures 3d-3g illustrate how the galvanic exchange process proceeds. Figure 3d shows the M$\mu$B-AgNP composite trapped at the WE. The first step in the detection process is the application of a voltage to the Au-modified WE. This results in conversion of $Au^0$ to $Au^{3+}$. A key feature of the *No*Slip is that this oxidant is formed exactly where it is required: adjacent to the trapped AgNPs. As mentioned

[2]Part of the text in this section has been adapted with permission from ACS Sensors 2016, 1, 40-47, DOI: 10.1021/acssensors.5b00051. Copyright 2016 the American Chemical Society.

earlier, the oxidizing power of $Au^{3+}$ is sufficient to oxidize AgNPs, but it is not so strong as to interact with other components of the *No*Slip or the matrix present in the channel (*e.g.*, blood or urine) [19]. Another important point is that even if biomolecules present in blood adsorb to the Au electrode during operation of the device, they will be instantaneously removed when the Au layer is oxidized, thereby presenting a virgin surface for subsequent detection of the AgNPs (described next).

Figure 3e shows that eq. 1 now proceeds spontaneously to yield $Ag^{+}$. A second 200 s voltage pulse results in electrodeposition of metallic Ag onto the surface of the working electrode (Figure 3f). In the last detection step (Figure 3g), metallic Ag is electrochemically oxidized using a simple electrochemical technique known as anodic stripping voltammetry (ASV). All of these electrochemical pulses and scans are automated by a dedicated reader. Integration of the area under the ASV peak corresponds to the charge contained in the AgNP labels, and hence it reflects the original concentration of the analyte. Importantly, in the absence of galvanic exchange no Ag signal is observed even at high AgNP concentrations. In other words, there is no direct oxidation of AgNPs at the working electrode, and therefore this galvanic exchange approach is a zero-background detection method.

A key aspect of the *No*Slip detection method is that it provides two stages of chemical amplification [23]–[25]. The first corresponds to a 20-fold preconcentration of the AgNP labels at the working electrode surface using magnetic force [26]. The second corresponds to the 250,000 equivalents of charge present in each 20 nm-diameter AgNP label. Combined, these two factors result in a 5 million-fold amplification of each bound target present in the sample. Moreover, the *No*Slip does not require enzymatic amplification of the type used in ELISA assays and most electrochemical sensors. Enzymes are sometimes fragile and are always slow, so the galvanic exchange detection strategy represents a significant advance over the current state of the art.

We collected ASVs after injecting different concentrations of the M$\mu$B-AgNP composite (in borate buffer) into *No*Slip sensors (Figure 4a). The *No*Slips are disposable, so each experiment was carried out using a different *No*Slip device. The observed shifts in ASV peak potentials are due to the nature of the (low-cost) reference electrode. This is not a problem for *No*Slip detection, however, because there are no other species oxidized within the potential range of the Ag ASV peak position. The dose-response curve in Figure 4b shows the relationship between charge (measured by integrating ASV peaks like those in Figure 4a) and AgNP concentration. Between 2.1 and 33.8 pM the plot is linear, but at higher AgNP concentrations the dose-response curve plateaus, suggesting that insufficient $Au^{3+}$ was created during the initial voltage pulse to fully oxidize the AgNPs during galvanic exchange. The important point, however, is that even at this very early stage of development, the pre-prototype *No*Slip is able to detect 2.1 pM of the AgNP labels in a chloride-containing buffer in just 7 min [19].

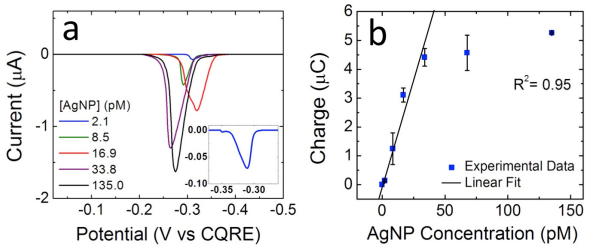


**FIGURE 4. Electrochemical ASV results for detection of the M$\mu$B-AgNP composite in borate buffered saline (100 mM borate, 100 mM NaCl, pH 7.5) solution using the *No*Slip. (a) ASVs recorded for the concentrations of AgNP labels shown in the legend. The inset shows an expanded view of the ASV obtained for 2.1 pM AgNPs. The scan rate was 0.010 V/s, and scans started at −0.70 V and ended at 0.20 V. The ASVs were corrected for a sloping baseline that results from oxygen reduction. (b) Calibration curve showing the correlation between charge (obtained by integrating ASVs like those in (a)) and the concentration of AgNPs. Each data point represents the average of at least three measurements carried out using independently fabricated *No*Slips. The error bars represent the standard deviation of those measurements. The black line is the best linear fit to the data points, weighted by the error bars. Reprinted with permission from *ACS Sensors* 2016, *1*, 40-47. (DOI: 10.1021/acssensors.5b00051). Copyright 2016 American Chemical Society.**

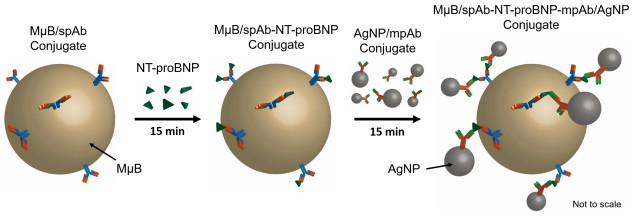


**FIGURE 5. Formation of the NT-proBNP immunocomposite.**

Unlike the model analyte, NT-proBNP is determined using a pair of antibodies (Abs). Abs specific to NT-proBNP were conjugated to 2.8 $\mu$m-diameter magnetic microbeads (M$\mu$B/spAb). We refer to these as the stationary phase Abs, though strictly speaking the microbeads are mobile. Abs specific to a different epitope of NT-proBNP (the mobile phase Abs) were conjugated to 20 nm-diameter AgNP labels (AgNP/mpAb) (Figure 5). As mentioned previously, AgNPs are used as labels because they are less sensitive to environmental changes than enzymes and provide a high degree of signal amplification quickly.

After an extensive literature search, it became apparent that the choice of Abs is crucial to sensing NT-proBNP. Different NT-proBNP assays have yielded different results for the same amount of endogenous NT-proBNP, and some of the discrepancies arise from the use of different Abs [27] while discrepancies between different assays using the same Abs are less understood [28], [29]. We found that Abs targeting glycosylated regions of NT-proBNP have qualitatively lower binding affinities towards endogenous NT-proBNP than Abs targeting non-glycosylated regions. Further, Abs that target the N-terminus of the analyte display less activity towards endogenous NT-proBNP, because the peptide is often truncated. As a result, and prior to embarking on our laboratory experiments, we researched, identified, and selected an Ab pair that targets non-glycosylated regions of NT-proBNP that are far enough away from one another to minimize steric

IEEE Journal of Translational Engineering in Health and Medicine

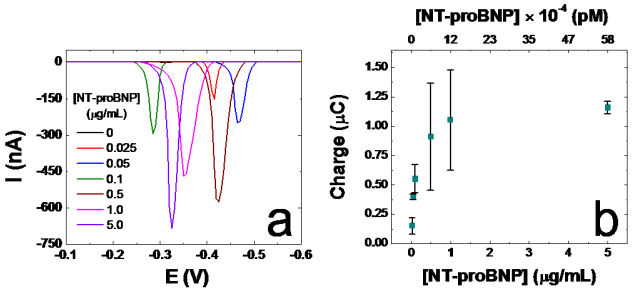


**FIGURE 6. Electrochemical ASV results for detection of the NT-proBNP immunocomposite in borate buffered saline (100 mM borate, 100 mM NaCl, pH 7.5) using the *No*Slip. (a) ASVs for the concentrations of NT-proBNP indicated in the legend. The scan rate was 0.060 V/s, and scans started at −0.70 V and ended at 0.20 V. The ASVs were corrected for a sloping baseline that results from oxygen reduction. (b) Calibration curve showing the correlation between charge (obtained by integrating ASVs like those in (a)) and the concentration of NT-proBNP. Each data point represents the average of at least three measurements carried out using independently fabricated *No*Slips. The error bars represent the standard deviation of those measurements. The data were treated using Dixon's Q test.**

repulsion, and that do not bind at the N-terminus of the peptide.

Our ultimate goal is to develop an assay platform wherein the user only has to input a sample, but at this early stage we prepared the NT-proBNP immunocomplex off-chip (Figure 5). The M$\mu$B/spAb conjugate was formed by reacting primary amines on the spAb (HyTest monoclonal anti-NT-proBNP 15C4) with epoxide groups present on the M$\mu$B. The AgNP/mpAb conjugate was prepared by physisorption of the mpAb (HyTest monoclonal anti-NT-proBNP 13G12) onto the 20 nm AgNPs. The spAb binds to amino acid residues 61-76 on NT-proBNP, and the mpAb binds to amino acid residues 13-27. Once the M$\mu$B/spAb and AgNP/mpAb reagents were prepared, they were used to form a M$\mu$B/spAb-NT-proBNP-mpAb/AgNP sandwich, which will be referred to henceforth as the 'immunocomposite'. The immunocomposite was prepared as follows. First, M$\mu$B/spAb and NT-proBNP were incubated in 100 mM aqueous borate (pH 7.5) for 15 min followed by washing three times in the borate solution. Second, the M$\mu$B/spAb-NT-proBNP complex was mixed with AgNP/mpAb and incubated for 15 min in the same borate solution. Finally, the sandwich immunocomposite was washed three times in the borate solution.

Once prepared, the immunocomplex was resuspended in 50 $\mu$L of borate-buffered saline (100 mM borate, 100 mM NaCl, pH 7.5) and injected into the inlet of the *No*Slip. When flow ceased, the electrochemical detection program was run. The assay results are shown in Figure 6. The ASVs in Figure 6a are similar to those shown in Figure 4a for the M$\mu$B-AgNP model composite. Figure 6b is a dose-response curve obtained by integrating the charges under the ASVs for at least three independent assays at each concentration and plotting as a function of the concentration of NT-proBNP. The shape of this plot is typical for ELISA-type assays, and the dynamic range is 2.9 - 582 nM.

### C. DISCUSSION

This dynamic range of the NT-proBNP assay is a little more than an order of magnitude higher than is required to meet the target of 53 – 590 pM. We are, however, quite confident that the assay range can be lowered appropriately for the following reasons. First, results for the M$\mu$B-AgNP composite (data summarized in Figure 4) indicate an LOD of 2.1 pM [19], which is more than an order of magnitude lower than our target range for NT-proBNP. This suggests that the preliminary NT-proBNP data are not device-limited, but are rather a function of either the Abs selected for the assay results shown in Figure 6 or the method used for their immobilization on the AgNPs and/or M$\mu$Bs. Second, optimization of the NT-proBNP assay is, at this early stage, far from complete in terms of both reagent and device configuration.

One other point is important to mention here. The coefficients of variation (CVs), represented by the error bars in Figure 6b, clearly require improvement. We believe this unacceptable level of variability originates from the fairly primitive *No*Slip holder and electrodes we are presently using, and also device-to-device variability resulting from our current one-device-at-a-time fabrication methods. These and other challenges, such as transitioning from buffer to human blood and incorporating the assay reagents on-chip, are presently being addressed in our labs.

## III. CONCLUSION

We have learned a tremendous amount about HF, home testing, NT-proBNP, and the entire health care ecosystem during the past two years. Here is a short list of lessons learned. First, there's a good reason why the vast majority of sensors for home testing are never deployed: the technological hurdles are daunting. Second, one needs to implement the practice of concurrent engineering throughout the development of a technology to avoid what can be the costly pitfalls of sequential or 'waterfall' development processes. Third, the technology is only part of the story, and inventors must also consider the customer(s) and the health economics case, the path to market, including manufacturability, and regulatory considerations very early in the process. This can only happen if the inventors spend time understanding the needs of all the stakeholders.

We have made significant of technical progress with the *No*Slip, but it still has operating characteristics we don't fully understand. These manifest as insufficient reproducibility, but we are getting very close to the levels necessary for human testing for NT-proBNP. Just two final points. First, we believe that in 10-20 years, home medical testing will be just as common as home-use Internet is today. Second, the *No*Slip form factor provides a template for other types of home testing that rely on Ab recognition of the target.

When combined with broader efforts in late-stage (T4) implementation science to streamline uptake of these innovations, POCTs, like the *No*Slip and other technologies within the broader digital health ecosystem, promise to markedly

change our approach to non-communicative disease detection and treatment throughout the world. Partnership among the scientific, non-profit, industrial, and governmental communities will be key as we continue to translate innovation into real-world application to turn discovery into markedly better health outcomes.

## ACKNOWLEDGMENT

The authors thank the organizers of the NIH-IEEE 2016 Strategic Conference on Healthcare Innovations and Point-of-Care Technologies for the opportunity to discuss emerging point-of-care technologies for HLBS diseases. They express their thanks to the American Chemical Society for permission to reproduce some of the material in this article.

## REFERENCES

[1] V. L. Roger, "Epidemiology of heart failure," *Circulat. Res.*, vol. 113, pp. 646–659, Aug. 2013.

[2] M. Federmann and O. M. Hess, "Differentiation between systolic and diastolic dysfunction," *Eur. Heart J.*, vol. 15, pp. 2–6, Dec. 1994.

[3] S. A. Hunt, "ACC/AHA 2005 guideline update for the diagnosis and management of chronic heart failure in the adult: A report of the American College of Cardiology/American Heart Association Task Force on Practice Guidelines (writing committee to update the 2001 guidelines for the evaluation and management of heart failure): Developed in collaboration with the American College of Chest Physicians and the International Society for Heart and Lung Transplantation: Endorsed by the Heart Rhythm Society," *Circulation*, vol. 112, pp. e154–e235, Sep. 2005.

[4] C. W. Yancy *et al.*, "2013 ACCF/AHA guideline for the management of heart failure," *J. Amer. College Cardiol.*, vol. 62, pp. e147–e239, Oct. 2013.

[5] J. Fang, G. A. Mensah, J. B. Croft, and N. L. Keenan, "Heart failure-related hospitalization in the U.S., 1979 to 2004," *J. Amer. College Cardiol.*, vol. 52, pp. 428–434, Aug. 2008.

[6] A. B. Cuyjet and O. Akinboboye, "Acute heart failure in the African American patient," *J. Cardiac Failure*, vol. 20, pp. 533–540, Jul. 2014.

[7] E. N. Eremin, A. N. Maltsev, and V. L. Syaduk, "Catalytic synthesis of ammonia in a barrier discharge," *Russ. J. Phys. Chem.*, vol. 45, no. 5, p. 635, 1971.

[8] V. Mukerji, "Dyspnea, orthopnea, and paroxysmal nocturnal dyspnea," in *Clinical Methods: The History, Physical, and Laboratory Examinations*, H. K. Walker, W. D. Hall, and J. W. Hurst, Eds. 3rd ed. Boston, MA, USA: Butterworths, 1990.

[9] M. Dewar and R. Curry, "Chronic obstructive pulmonary disease: Diagnostic considerations," *Amer. Family Phys.*, vol. 73, no. 4, pp. 669–676, 2006.

[10] M. Dolgin and New York Heart Association Criteria Committee, *Nomenclature and Criteria for Diagnosis of Diseases of the Heart and Great Vessels*, 9th ed. Boston, MA, USA: Little, Brown and Company, 1994.

[11] H.-N. Kim and J. L. Januzzi, "Natriuretic peptide testing in heart failure," *Circulation*, vol. 123, pp. 2015–2019, May 2011.

[12] T. Mueller, A. Gegenhuber, B. Dieplinger, W. Poelz, and M. Haltmayer, "Long-term stability of endogenous B-type natriuretic peptide (BNP) and amino terminal proBNP (NT-proBNP) in frozen plasma samples," *Clin. Chem. Lab. Med.*, vol. 42, pp. 942–944, Aug. 2004.

[13] J. L. Januzzi *et al.*, "The N-terminal Pro-BNP investigation of dyspnea in the emergency department (PRIDE) study," *Amer. J. Cardiol.*, vol. 95, pp. 948–954, Apr. 2005.

[14] J. L. Januzzi, "NT-proBNP testing for diagnosis and short-term prognosis in acute destabilized heart failure: An international pooled analysis of 1256 patients: The international collaborative of NT-proBNP Study," *Eur. Heart J.*, vol. 27, pp. 330–337, Nov. 2005.

[15] S. Anwaruddin *et al.*, "Renal function, congestive heart failure, and amino-terminal pro-brain natriuretic peptide measurement: Results from the ProBNP investigation of dyspnea in the emergency department (PRIDE) study," *J. Amer. College Cardiol.*, vol. 47, pp. 91–97, Jan. 2006.

[16] A. Bayes-Genis *et al.*, "Effect of body mass index on diagnostic and prognostic usefulness of amino-terminal pro–brain natriuretic peptide in patients with acute dyspnea," *Arch. Internal Med.*, vol. 167, no. 4, pp. 400–407, 2007.

[17] J. L. Januzzi and R. Troughton, "Are serial BNP measurements useful in heart failure management?" *Circulation*, vol. 127, no. 4, pp. 500–508, 2013.

[18] A. W. Martinez, S. T. Phillips, M. J. Butte, and G. M. Whitesides, "Patterned paper as a platform for inexpensive, low-volume, portable bioassays," *Angew. Chemie Int. Ed.*, vol. 46, pp. 1318–1320, Feb. 2007.

[19] J. C. Cunningham, M. R. Kogan, Y.-J. Tsai, L. Luo, I. Richards, and R. M. Crooks, "Paper-based sensor for electrochemical detection of silver nanoparticle labels by galvanic exchange," *ACS Sens.*, vol. 1, no. 1, pp. 40–47, 2016.

[20] C. Renault, X. Li, S. E. Fosdick, and R. M. Crooks, "Hollow-channel paper analytical devices," *Anal. Chem.*, vol. 85, no. 16, pp. 7976–7979, 2013.

[21] C. Renault, J. Koehne, A. J. Ricco, and R. M. Crooks, "Three-dimensional wax patterning of paper fluidic devices," *Langmuir*, vol. 30, no. 23, pp. 7030–7036, 2014.

[22] A. J. Bard and L. R. Faulkner, *Electrochemical Methods*, 2nd ed. New York, NY, USA: Wiley, 2001.

[23] X. Li, K. Scida, and R. M. Crooks, "Detection of hepatitis B virus DNA with a paper electrochemical sensor," *Anal. Chem.*, vol. 87, pp. 9009–9015, Aug. 2015.

[24] J. C. Cunningham, K. Scida, M. R. Kogan, B. Wang, A. D. Ellington, and R. M. Crooks, "Paper diagnostic device for quantitative electrochemical detection of ricin at picomolar levels," *Lab Chip*, vol. 15, no. 18, pp. 3707–3715, 2015 2015.

[25] K. Scida, J. C. Cunningham, C. Renault, I. Richards, and R. M. Crooks, "Simple, sensitive, and quantitative electrochemical detection method for paper analytical devices," *Anal. Chem.*, vol. 86, no. 13, pp. 6501–6507, 2014.

[26] J. C. Cunningham, P. R. DeGregory, and R. M. Crooks, "New functionalities for paper-based sensors lead to simplified user operation, lower limits of detection, and new applications," *Annu. Rev. Anal. Chem.*, vol. 9, pp. 183–202, Jul. 2016.

[27] K. R. Seferian *et al.*, "Immunodetection of glycosylated NT-proBNP circulating in human blood," *Clin. Chem.*, vol. 54, no. 5, pp. 866–873, 2008.

[28] A. Clerico *et al.*, "State of the art of BNP and NT-proBNP immunoassays: The CardioOrmoCheck study," *Clin. Chim. Acta*, vol. 414, pp. 112–119, Dec. 2012.

[29] K. N. Luckenbill *et al.*, "Cross-reactivity of BNP, NT-proBNP, and proBNP in commercial BNP and NT-proBNP assays: Preliminary observations from the IFCC committee for standardization of markers of cardiac damage," *Clin. Chem.*, vol. 54, pp. 619–620, Mar. 2008.

**Authors'** photographs and biographies not available at the time of publication.